Journal of Mechanics Engineering and Automation 11 (2021) 121-134
doi: 10.17265/2159-5275/2021.05.002

Study on Welding-Bead Bonding Strength of Laser-Stacking Copper-Aluminum Heterogeneous Electrode Plates

Shang-Wu Tsai[1], Shih-Kai Chien[2], Kun-Tso Chen[2], Tsung-Ying Tsai[2] and Wen-Cheng Tseng[3]

1. Computer Aided Engineering Center, Automotive Research and Testing Center (ARTC), Lukang Township, Changhua County 50544, Taiwan

2. Laser and Additive Manufacturing Technology Center, Industrial Technology Research Institute (ITRI), Tainan City 73445, Taiwan

3. Elite Crown Software and Consulting Co., Ltd., San Chung City Taipei County 24143, Taiwan

Abstract: In this paper, two types of copper-aluminum heterogeneous electrode plates are stacked and the finite element analysis (FEA) models of two different laser welding conditions are built by using SYSWELD welding simulation software to calculate the depth of the welding bead and the temperature distribution of the welding surface. Then, the residual stress analysis data of the welded area are exported and the residual stress is applied to the welded specimen for CAE analysis to ensure that the welding bonding strength meets the design target of a shear force of 500 N or higher. The copper-aluminum laser-stacking simulation technique in this paper can be applied to the manufacturing of copper-aluminum heterogeneous laser-welded electrodes and series-connected electrodes of automotive lithium-ion power battery modules, providing an effective analysis method for welding bonding-strength.

Key words: Copper-aluminum heterogeneous laser welding simulation, welding bonding strength analysis, finite element method.

1. Preface

Awareness of saving energy and carbon reduction has been increasing in recent years, while all major automakers and parts suppliers worldwide are committed to the development of electric vehicles (EVs), for which one of the key technologies is the power battery.

Lithium-ion batteries are becoming the mainstream of energy storage applications, thanks to high energy density, high reusability, and environmental friendliness. Generally speaking, energy storage systems are often achieved by connecting multiple lithium-ion battery cells in series and parallel, and the cells release lithium-ions through the positive and negative electrode materials to form a mechanism for storing and releasing electrical energy. Currently, major cathode materials include lithium iron phosphate ($LiFePO_4$), lithium ternary (NCM), and lithium manganese ($LiMnO_2$), which are designed in series or/and parallel by different EV makers according to the performance requirements of targeted vehicle models.

With the advantages of high reliability, high efficiency, narrow welding bead and low thermal impact, the introduction of laser welding technology into lithium-ion battery manufacturing is expected to significantly improve product quality and production efficiency. Particularly in response to demand for laser-welding manufacturing of soft-pack batteries, it is key to well control the width, depth, and bonding strength of the welding beads, as it is common to have different thicknesses of copper and aluminum heterogeneous plates stacked between the battery electrodes and each cell (Bus bar or Tab).

This paper tries to: set up the FEA models for two types of laser-stacked welding of copper and aluminum heterogeneous electrode sheets, analyze the width and depth of the welding bead and the

Corresponding author: Shang-Wu Tsai, Ph.D. in mechanical engineering, research fields: fracture mechanics, finite element analysis and structure mechanics.

temperature of the welding surface, and compare them with experimental results.

Then, the residual-stress data of the welded area are exported and the residual stress is applied to the welded specimen for weld bonding-strength simulation to ensure that the laser welding bonding-strength meets the design target of a shear force of more than 500 N and to verify its accuracy with the relevant laser welding tests. The bonding strength analysis of the stacked electrode plates in this paper is expected to provide an effective welding bonding-strength analysis method for different welding conditions, and speed up the development while experimental-error costs are saved.

2. Finite Element Heat-Source Modeling of Copper-Aluminum Heterogeneous Laser-Stacking Welding

In this section, we use SYSWELD welding simulation software to build a finite element heat-source model and use the model to simulate the width, depth and temperature distribution of laser welding. The two types of copper-aluminum (Cu-Al) heterogeneous stacking and welding conditions are described as below:

(1) Stacking type of upper layer aluminum (1050) and lower layer copper (C1100):

Copper specimen size: 60 mm (L) 20 mm (W) 1.0 mm (H); aluminum specimen size: 60 mm (L) 20 mm (W) 0.5 mm (H). The laser welding conditions include: laser heat-source power 2,000 W, laser scanning speed 275 mm/s, laser path 10 mm straight, and spot size 0.12 mm (120 μm), as shown in Fig. 1.

(2) Stacking type of upper copper (C1100) and lower aluminum (1050):

Copper specimen size: 60 mm (L) 20 mm (W) 0.5 mm (H); aluminum specimen size: 60 mm (L) 20 mm (W) 1.0 mm (H). The laser welding conditions: laser heat-source power 1,500 W, laser scanning speed 225 mm/s, laser path 10 mm straight, and spot size 0.12 mm (120 μm), as shown in Fig. 1.

Regarding the finite element heat-source modeling (see Fig. 1), the thickness of the upper and lower layer (either Cu or Al) of the specimen is 0.5 mm and 1 mm, respectively. The element type is three-dimensional hexahedral elements, and the element size is controlled to be about 0.04 mm in the welding-bead area, while graded outward to about 1 mm. Total number of elements is 87,395, as shown in Fig. 2. Then the model is built under material properties of red brass C1100 and aluminum 1050; while the physical properties are shown in Table 1. The thermal and stress strain curves under different temperatures are shown in Figs. 3 and 4, respectively.

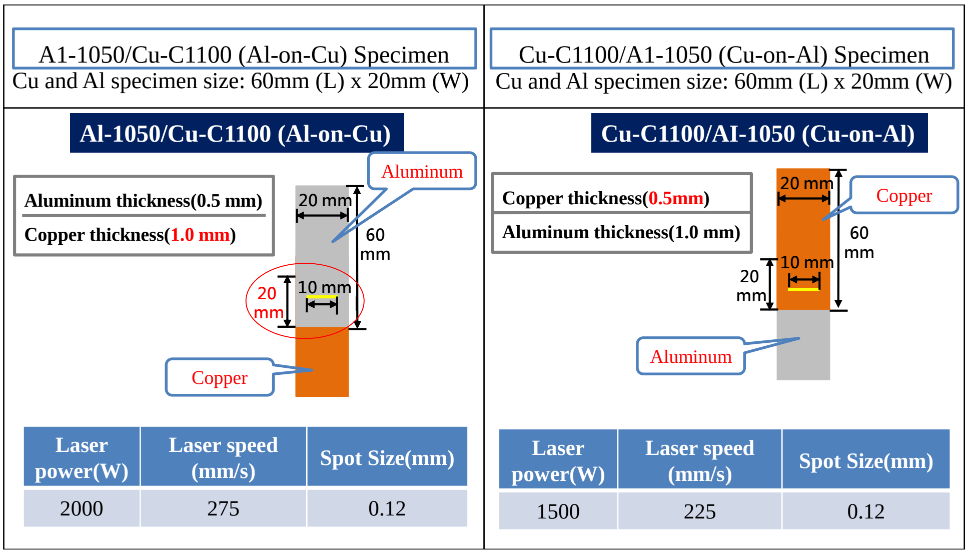

Fig. 1 Welding conditions for Cu-Al heterogeneous materials.

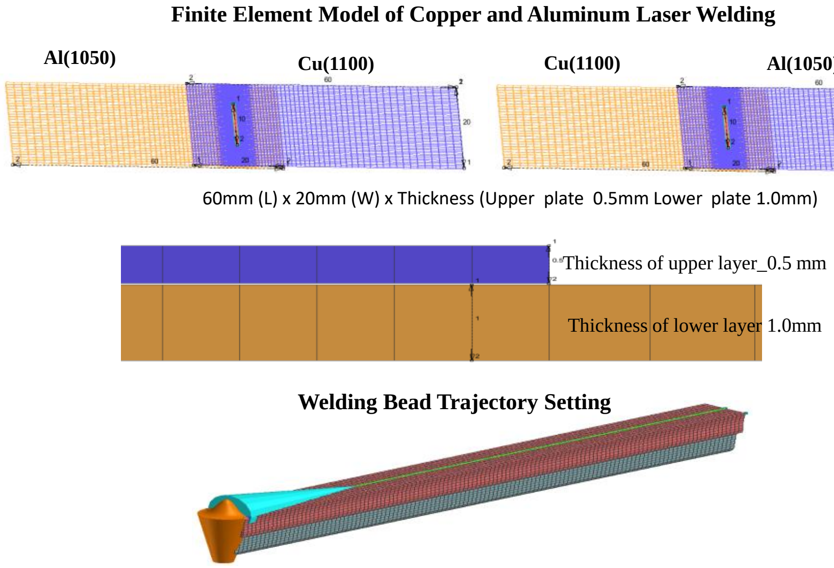

Fig. 2 FEA modeling of laser heat-source.

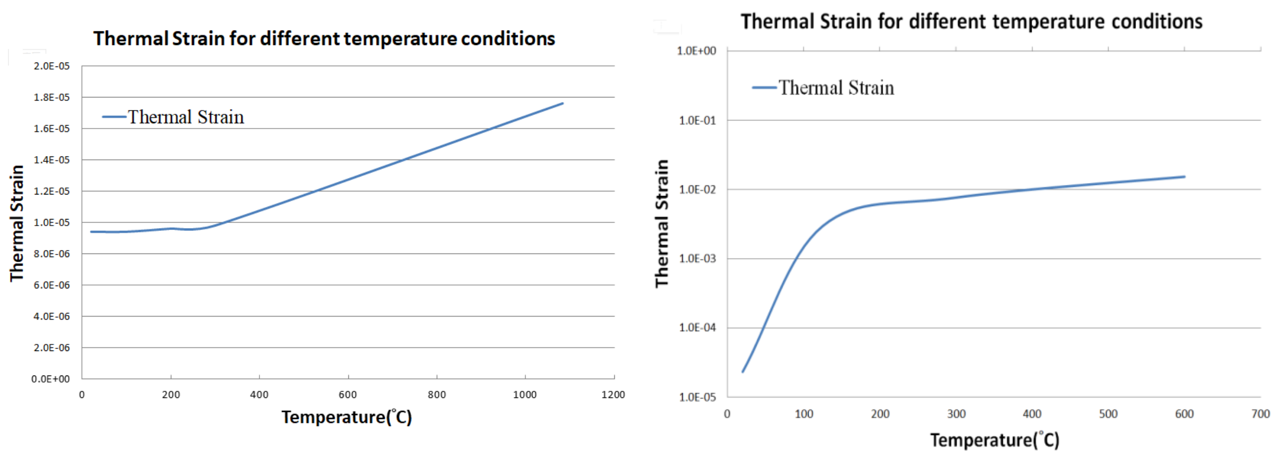

Copper C1100 Aluminum 1050

Fig. 3 Thermal strain curves of copper C1100 and aluminum 1050 at different temperatures.

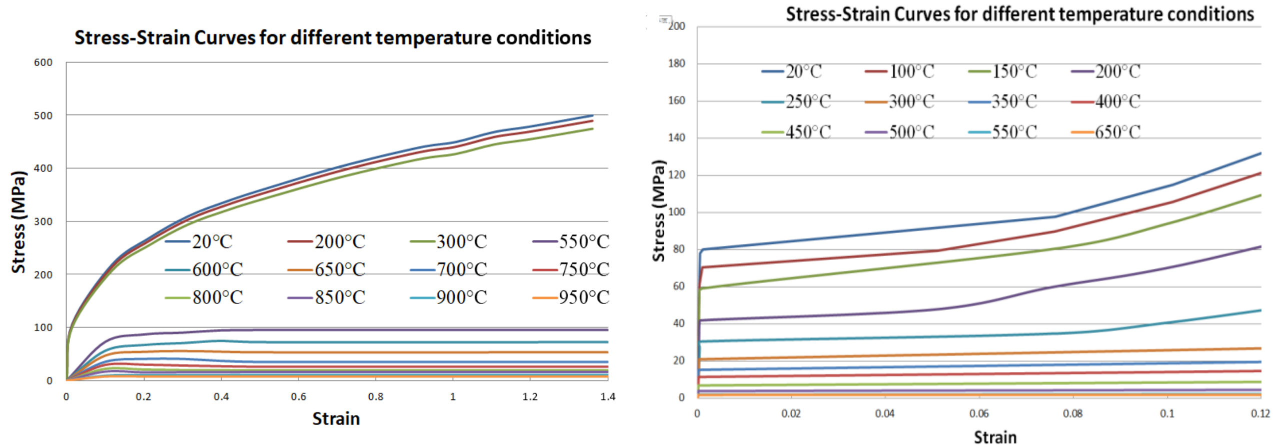

Copper C1100 Aluminum 1050

Fig. 4 Stress-strain curves of copper C1100 and aluminum 1050 at different temperatures.

Table 1 Material physical properties.

Mechanical properties	Copper (C1100)	Aluminum (1050)
Young's modulus (MPa)	117,211	68,900
Poisson's ratio	0.34	0.33
Material density (kg/mm^3)	8.94×10^{-6}	2.73×10^{-6}
Thermal strain under different temperatures	As shown in Fig. 3	As shown in Fig. 3
Stress-strain curve under different temperatures	As shown in Fig. 4	As shown in Fig. 4

3. Analysis of Molten-Pool Shape of Cu-Al Heterogeneous Laser-Stacking Welding Bead

The molten-pool shape and surface-temperature distribution of the laser-stacking welding beads (Cu-on-Al and Al-on-Cu) are calculated using above-mentioned finite element heat-source model [1, 2] in this paper.

The shapes of the molten pools of the Cu-Al heterogeneous electrodes are shown in Figs. 5 and 6, respectively. As shown in Fig. 5, when the specimen is stacked (Cu-on-Al) with laser power of 2,000 W, and the scanning speed is 275 mm/s, the welding depth of the welding-bead molten-pool shape is 0.964 mm, and the upper-surface welding width is 0.792 mm while welding width of the interface in-between upper and lower layers is 0.528 mm.

In Fig. 6, when the specimen is stacked (Al-on-Cu) with laser power of 1,500 W, and the scanning speed is 225 mm/s, the welding depth of the welding-bead molten-pool shape is 0.849 mm; and the upper-surface welding width is 0.502 mm; while welding width of the interface in-between upper and lower layers is 0.422 mm.

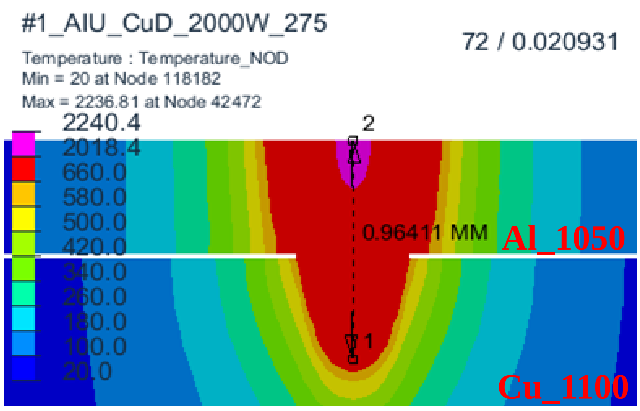

Laser welding depth analysis

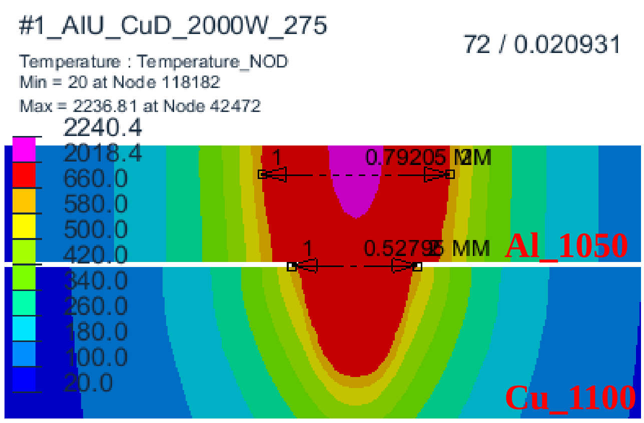

Laser welding width analysis

Fig. 5 CAE analysis of the molten-pool of laser welding (Al-on-Cu type).

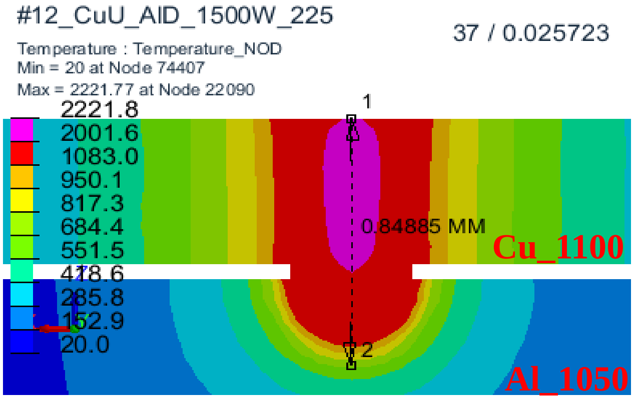

Laser welding depth analysis

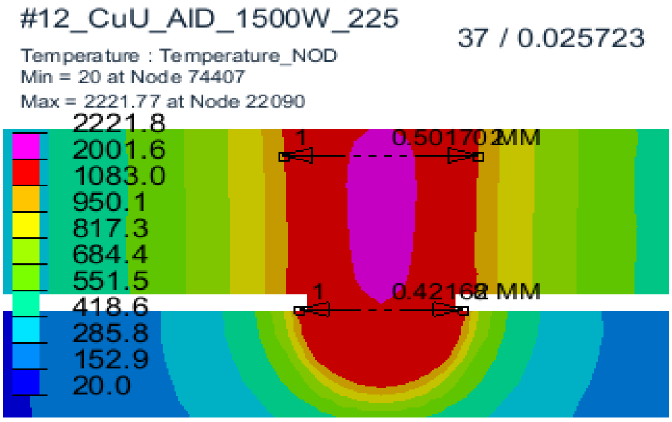

Laser welding width analysis

Fig. 6 CAE analysis of the molten-pool of laser welding (Cu-on-Al type).

The results of the cross-sectional metallographic tests for laser welding-beads are shown in Fig. 7, which are three sets of metallographic tests for each of the two types of laser-stacking welding conditions.

As shown in Table 2, the maximum error between the simulated and tested results for laser-stacking welding depth is 9.82%, which occurs when the laser-welding power is 2,000 W for the Al-on-Cu stacked type. The maximum error between the simulated and tested results for the welding width of laser welding is 12.83%, which occurs in the interface welding width of the 1,500 W Cu-on-Al stacked type. The comparison error is within 15% to ensure the correctness of the analytical model.

The simulated results of the welded surface temperature are compared with the measurement results of the thermal radiation wide-field sensing system, as shown in Fig. 8. The values of the surface-temperature measurement points are 540 ℃ and 672 ℃ for the laser power of 2,000 W (Al-on-Cu) and 1,500 W (Cu-on-Al), respectively.

From Table 3, it can be seen that the maximum error in the temperature field is the 1,500 W Cu-on-Al stacked type (11.63% in the comparison). The error values are within 15% to ensure the correctness of the finite element heat-source model.

4. Residual Stress and Deformation Analysis of Cu-Al Heterogeneous Laser-Stacking Welding Bead

After confirming the finite element heat-source model is correct for the simulations and tests, the information on the residual stress and deformation in the heat-affected zone of welding is output for the subsequent simulation analysis of weld-bonding strength [3-5]. The analyses of the residual stresses in

Control Factors		
Laser Power	Processing Speed	Scan Pass
W	mm/s	N
2000	275	1

Avg.
Top width : 799.3μm
Welding width : 479.7μm
Welding depth :1068.7μm

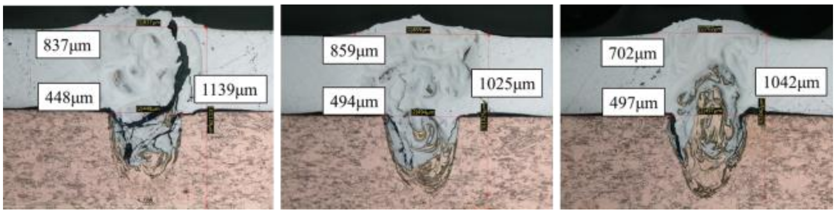

Al-on-Cu

Control Factors		
Laser Power	Processing Speed	Scan Pass
W	mm/s	N
1500	225	1

Avg.
Top width : 533.3μm
Welding width : 374.3μm
Welding depth :777.0μm

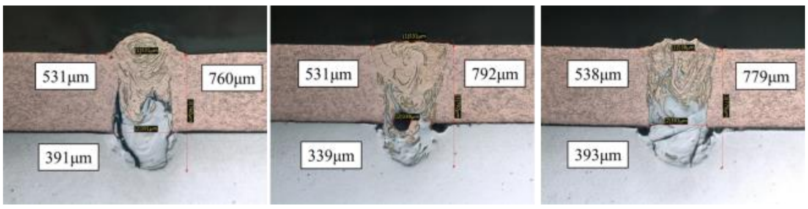

Cu-on-Al

Fig. 7 Metallographic section tests of welding beads.

Table 2 Simulation/experiment comparison of width & depth of Cu-Al heterogeneous laser welding.

Specimen-stacking type		Al-on-Cu	Cu-on-Al
Laser power (W)		2,000	1,500
Welding depth	CAE (mm)	0.964	0.849
	EXP. (mm)	1.069	0.777
	Error (%)	9.82	9.27
Welding width on upper surface	CAE (mm)	0.792	0.502
	EXP. (mm)	0.799	0.533
	Error (%)	0.88	5.82
Welding width on in-between interface	CAE (mm)	0.528	0.422
	EXP. (mm)	0.480	0.374
	Error (%)	10.00	12.83

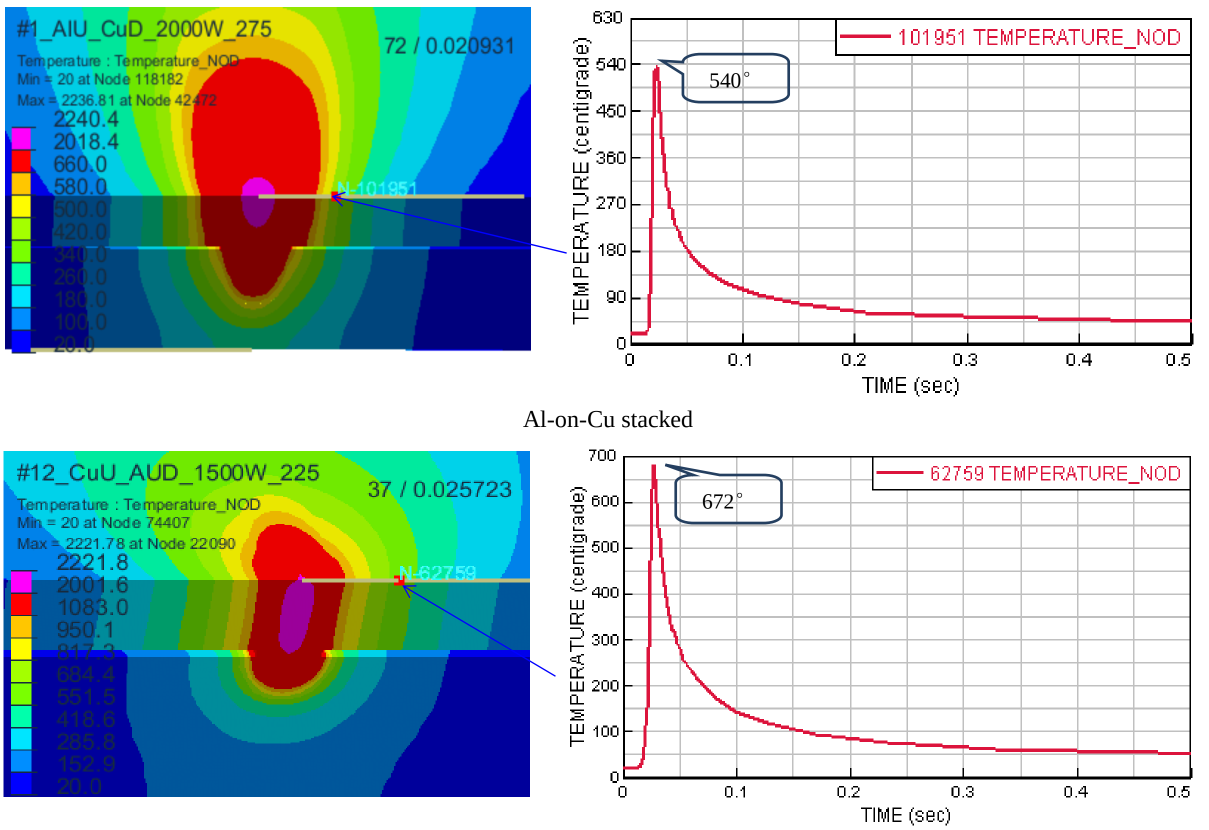

Al-on-Cu stacked

Cu-on-Al stacked

Fig. 8 CAE analysis of laser-welding temperature field.

Table 3 Analysis/experiment comparison of laser welding surface temperature field.

Specimen-stacking type		Al-on-Cu	Cu-on-Al
Laser power (W)		2,000	1,500
	CAE (℃)	540	672
Surface temperature(℃)	EXP. (℃)	504	602
	Error (%)	7.14	11.63

heat-affected area for the two types of laser-stacking welding are shown in Figs. 9 and 10, and the results of the deformation analysis are shown in Figs. 11 and 12, respectively.

As shown in Fig. 9, when the specimens are Al-on-Cu stacked, the maximum equivalent residual stress in the welding-bead occurs at the lower edge of the welding-bead of copper specimen (under conditions of laser power 2,000 W and scanning speed 275 mm/s), and the value is 118.5 MPa. From the analysis, the reason (maximum equivalent residual stress occurs at the welding-bead's lower edge) is because copper absorbs heat faster than aluminum (copper thermal conductivity: 391 W/(m K); aluminum thermal conductivity: 210 W/(m K)); and the copper's density is higher, leading to the heat being concentrated at the lower edge of the welding bead of the copper specimen.

When entering into the heat-dissipating stage, the thermal expansion coefficient of aluminum is larger than that of copper (Al: 2.32×10^{-5} 1/℃; Cu: 9.40×10^{-6} 1/℃), the thermal expansion deformation will squeeze the aluminum specimen to copper, causing the stress to be concentrated at the lower edge of the welding-bead of the copper specimen, and the corresponding residual stress value is also the largest [6-8].

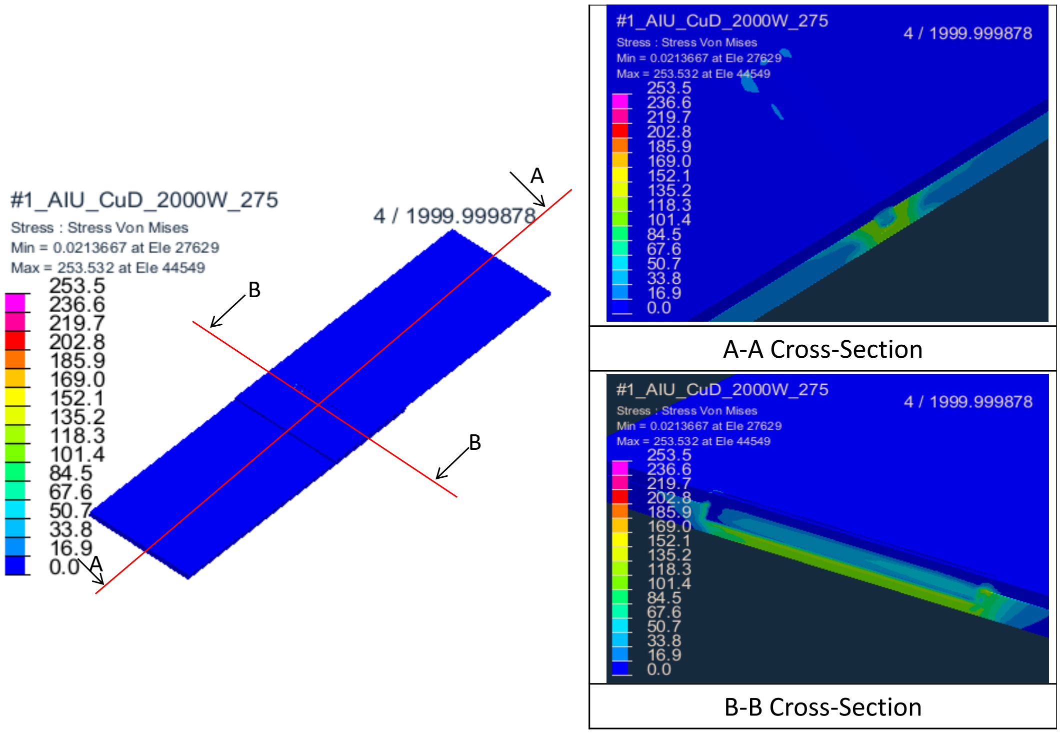

von-Mises stress analysis of welding-bead cross-section

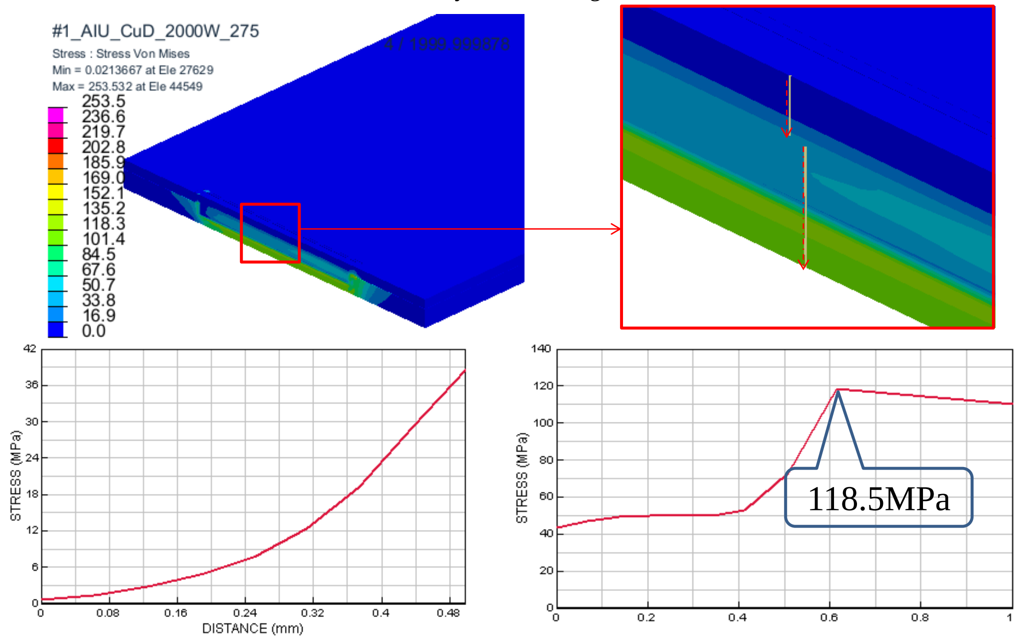

(a) von-Mises stress distribution (along thickness) of Al. upper-layer's welding-bead

(b) von-Mises stress distribution (along thickness) of Cu. lower-layer's welding-bead

von-Mises stress distribution (along thickness) of welding-bead center-section

Fig. 9 Residual stress analysis of laser-stacking welding-bead (Al-on-Cu).

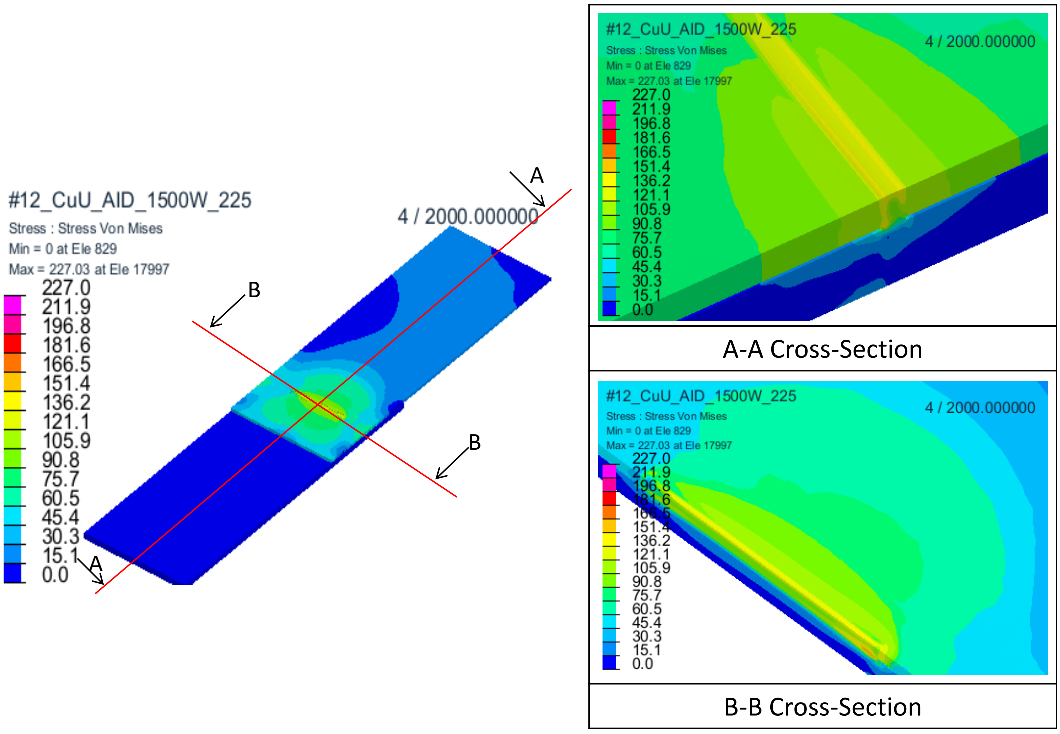

von-Mises stress analysis of welding-bead cross-section

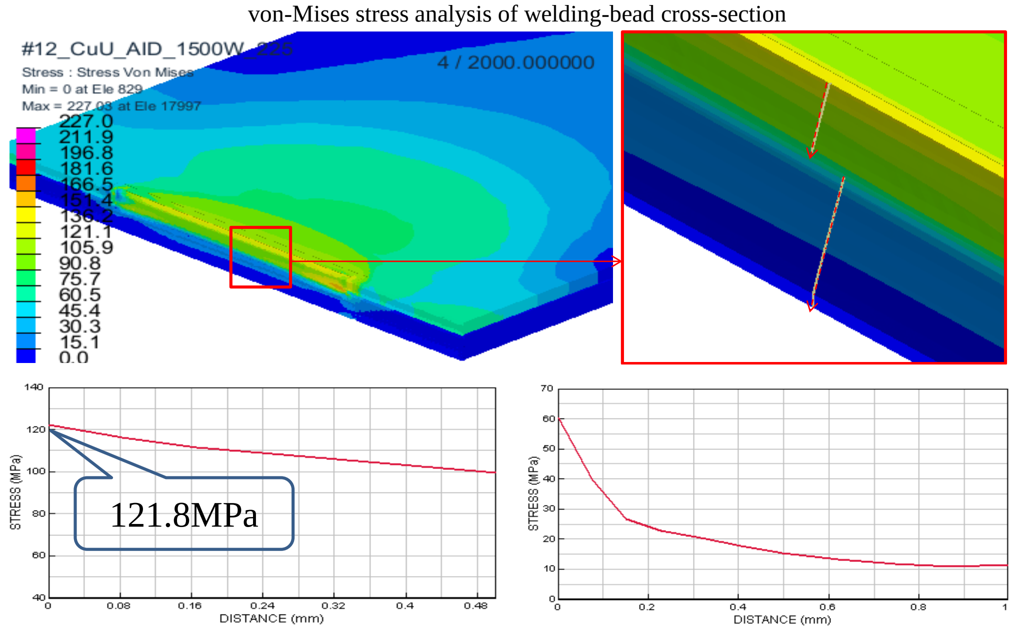

(a) von-Mises stress distribution (along thickness) of Cu. upper-layer's welding-bead

(b) von-Mises stress distribution (along thickness) of Al. lower-layer's welding-bead

von-Mises stress distribution (along thickness) of welding-bead center-section

Fig. 10 Residual stress analysis of laser-stacking welding-bead (Cu-on-Al).

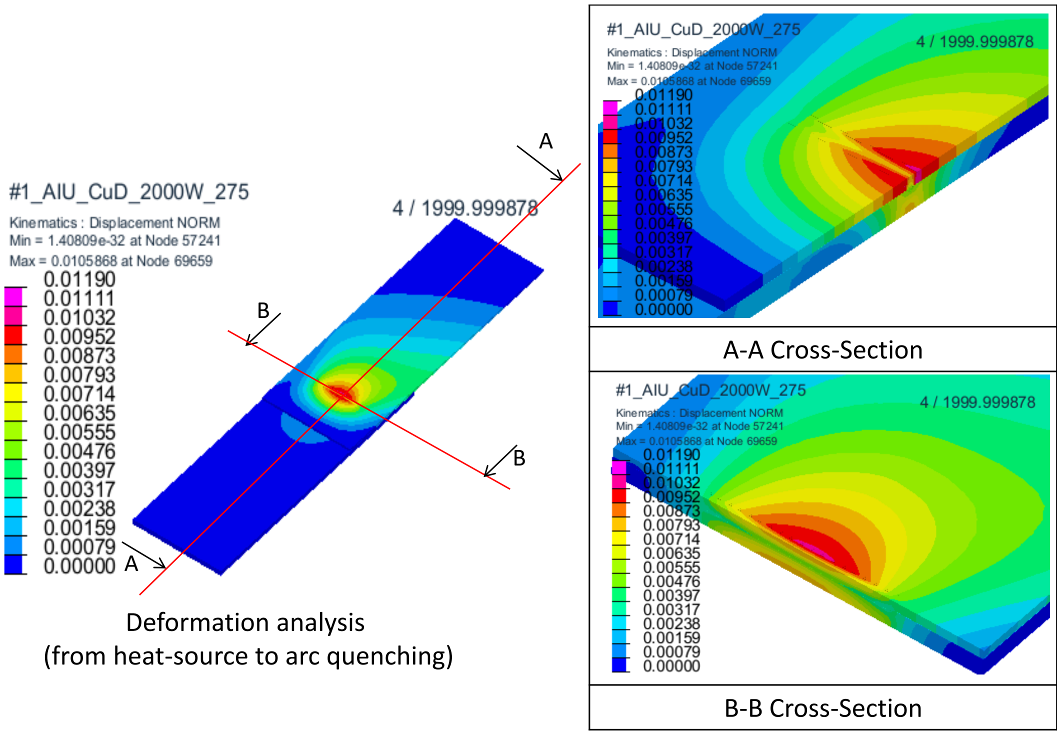

Fig. 11 Deformation analysis of laser-stacking welding-bead (Al-on-Cu).

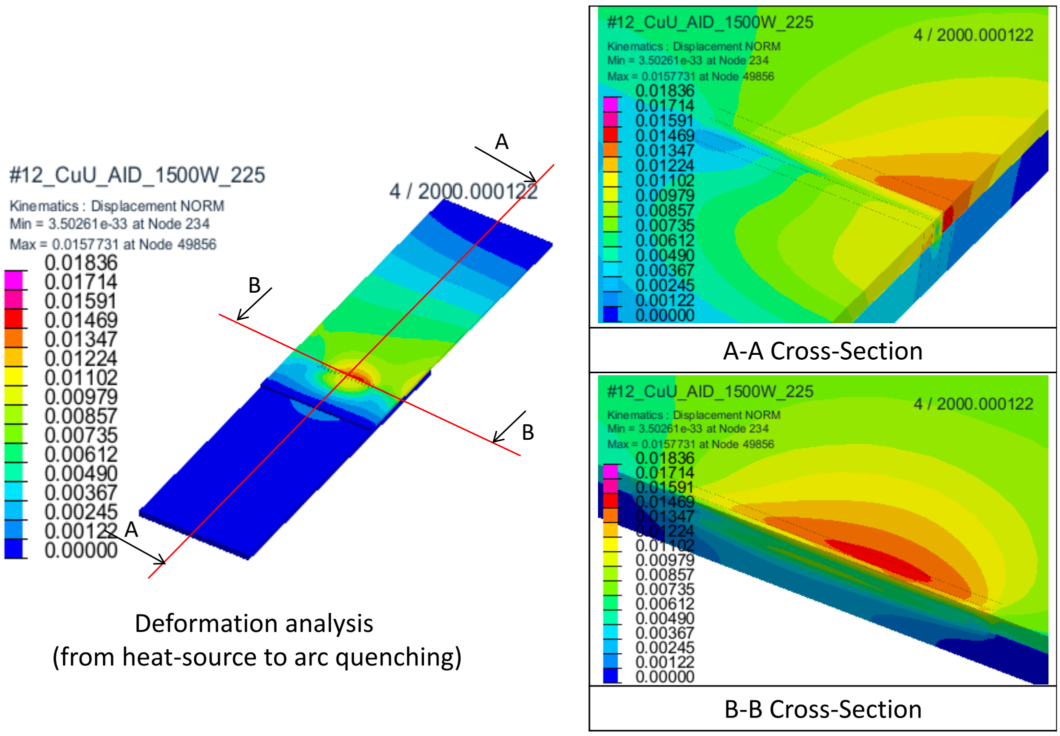

Fig. 12 Deformation analysis of laser-stacking welding-bead (Cu-on-Al).

In Fig. 10, when the specimens are stacked in Cu-on-Al type, with a laser power of 1,500 W and scanning speed of 225 mm/s, the maximum equivalent residual stress in the welding bead occurs at the top surface of the upper copper specimen, at 121.8 MPa. The analysis shows that the maximum equivalent residual stress is concentrated on the upper surface of the upper copper specimen, because the laser energy is transferred from the upper surface of the copper specimen to the lower aluminum specimen, while the upper surface of the copper specimen absorbs more heat capacity, leading to the heat being concentrated at the welding bead of the copper specimen. As the heat-dissipating stage, the heat-expansion coefficient of aluminum is larger than that of copper, the heat-expansion deformation will squeeze the aluminum specimen to copper, causing the stress to be concentrated on the top surface of the copper specimen, and the corresponding residual stress value will be the largest.

In Fig. 11, when the specimens are stacked Al-on-Cu, the maximum deformation of the molten pool cross-section is 11.90 μm at the location of the upper surface of the welding-bead where the laser hits the aluminum specimen. As shown in Fig. 12, when the specimen is stacked Cu-on-Al, the maximum deformation of the molten pool cross-section is 18.36 μm (laser power of 1,500 W), which occurs at the upper surface of the welding-bead of the copper specimens.

5. Simulation and Experimental Verification of Laser-Stacking Welding-Bead Bonding Strength

Inputting mentioned welding-bead residual-stress analysis results into the LS-DYNA software as the initial stress conditions for simulating the welding-bead bonding-strength (of laser-stacked Cu-Al heterogeneous electrode plates), the FEA model is shown in Fig. 13. The model is constructed for two different types of

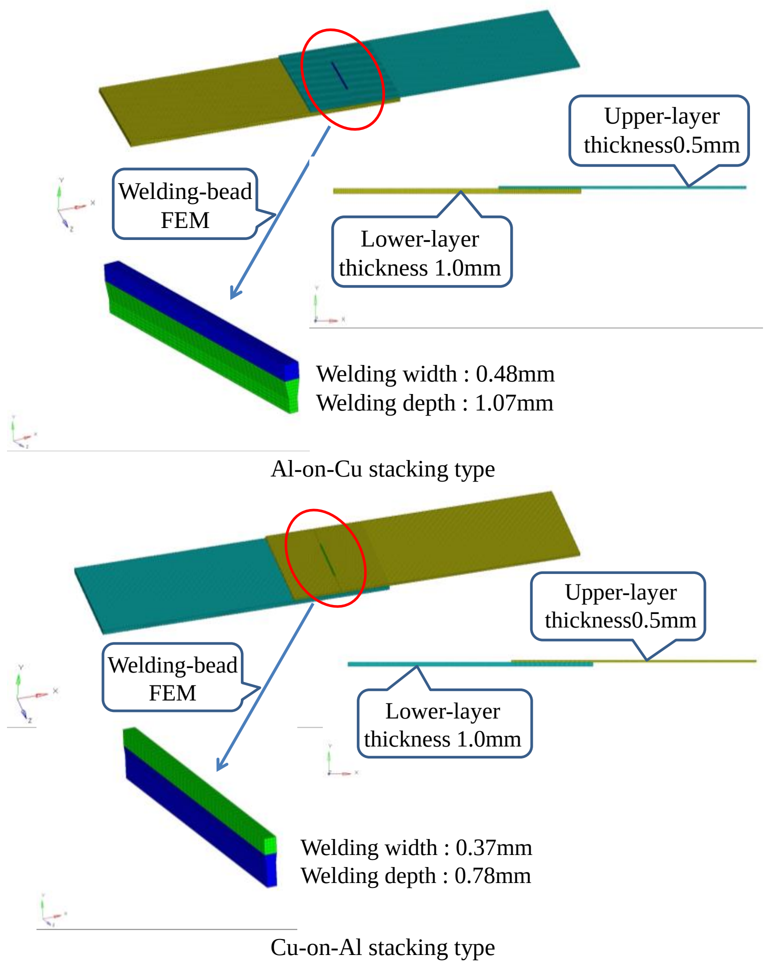

Fig. 13 Finite element modeling of Cu-Al heterogeneous laser-welding bonding strength.

welding-bead shapes of Cu-Al heterogeneous stacking. The thickness of the upper and lower layer is 0.5 mm and 1 mm, respectively. The element size is controlled from 0.06 mm to 0.20 mm; and the element types are 3D elements (Hexa Elements). Total number of elements in the models is 482,400 for the Al-on-Cu stacking and 400,800 for Cu-on-Al.

The laser-welding bonding-strength analysis conditions are illustrated in Fig. 14, where a fixed boundary condition is set for the lower-layer end, and a compulsory displacement is applied to one side of the upper layer. Analysis results are shown in Fig. 15, which indicates that the maximum shear forces of the Al-on-Cu stacking at laser power 2,000 W, and the Cu-on-Al at laser power of 1,500 W, are 618.29 N and 595.81 N, respectively. The welding shear force increases in conjunction with the welding depth (aluminum-on-copper stacking: 1.07 mm; copper-on-aluminum stacking: 0.78 mm).

The simulated welding bonding-strength and test results are compared and shown in Table 4, which indicate that the maximum shear force comparison error is 5.73% for the Cu-on-Al stacking with laser power of 1,500 W, and the error values are within 10%.

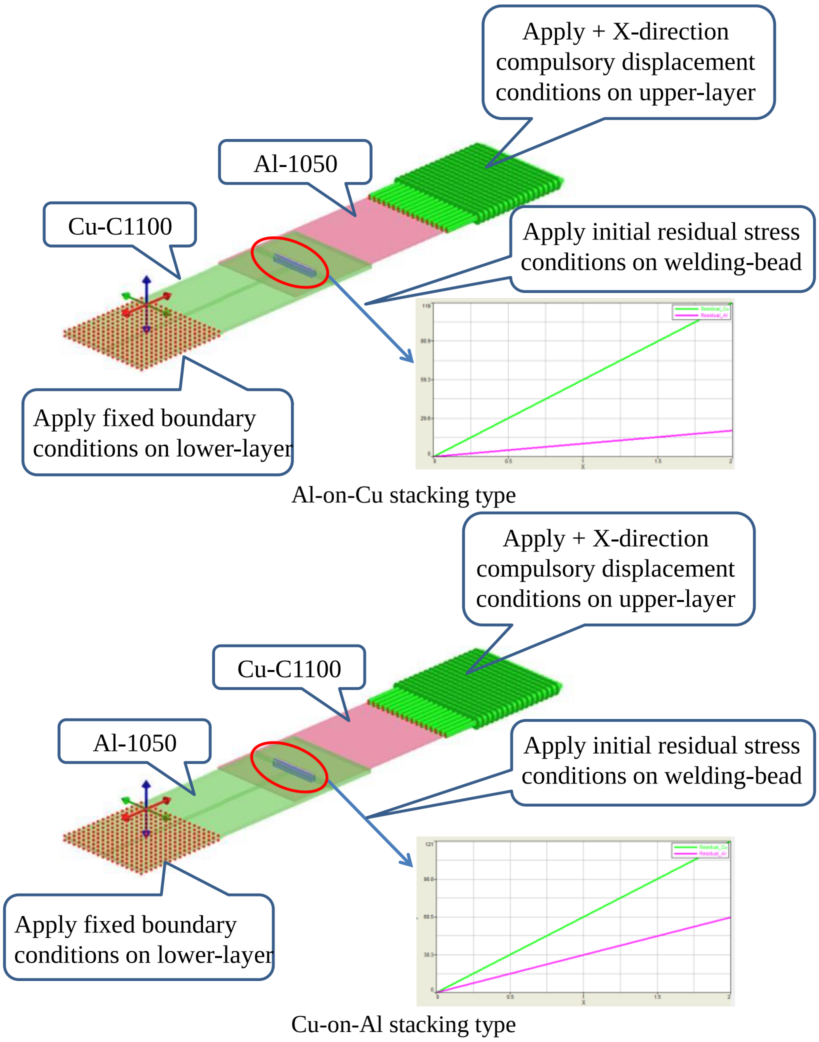

Fig. 14 Conditions for Cu-Al heterogeneous laser-welding bonding-strength analysis.

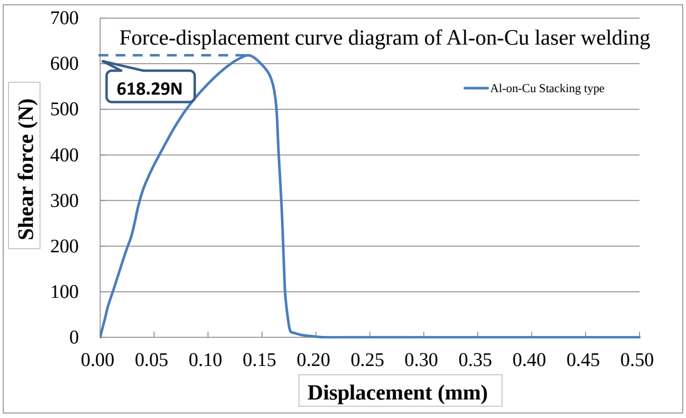

Al-on-Cu stacking type

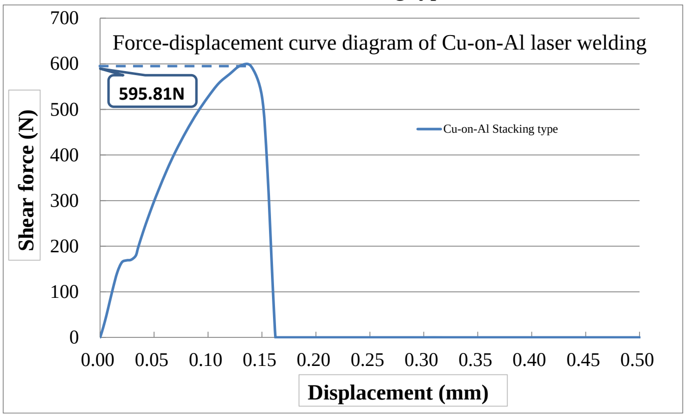

Cu-on-Al stacking type

Fig. 15 Bonding-strength analysis of Cu-Al heterogeneous laser welding.

Table 4 Bonding-strength of Cu-Al heterogeneous laser welding.

Specimen-stacking type	Al-on-Cu	Cu-on-Al
Laser power (W)	2,000	1,500
CAE (N)	618.29	595.81
EXP. (N)	591.50	563.50
Error (%)	4.53	5.73

6. Results and Discussion

In this paper, two types of Cu-Al heterogeneous electrode plates are analyzed for laser-stacking welding, and the finite element heat-source model is first established by using SYSWELD software. Then, the simulation analysis of the molten-pool shapes and temperature distributions of the welding-beads are compared with the experimental measurement results, followed by the simulation analysis and experimental verification of the bonding strength of the laser-stacking welding-beads.

The simulated analysis results of the molten-pool shape of laser welding include: welding depth (0.964 mm for Al-on-Cu stacking type; 0.849 mm for the Cu-on-Al); welding width of the upper surface (0.792 mm and 0.502 mm); and the welding width of the upper and lower interface (0.528 mm and 0.422 mm).

The results of the metallographic test of the welding-bead cross-section include: welding depth (1.069 mm for Al-on-Cu, 0.777 mm for Cu-on-Al); welding width of the upper surface (0.799 mm and 0.533 mm); and the welding width of the interface (in-between upper and lower (0.480 mm and 0.374 mm).

Comparison accuracy of the simulated and tested welding molten-pool shape is within 15%, assuring the correctness of the finite element heat-source model.

The experimental measurement data of the thermal radiation wide-field sensing system are 504 ℃ for Al-on-Cu type and 602 ℃ for Cu-on-Al; and the comparison error with CAE analysis is within 15% (540 ℃ and 672 ℃) assuring the correctness of the constructed finite element heat-source model.

In simulation analysis of bonding strength of laser-stacking welding-beads: From CAE analysis, the maximum shear force value is 618.29 N for Al-on-Cu and 595.81 N for Cu-on-Al, which is in accordance with the design target of higher than 500 N.

The maximum shear force is 591.50 N for Al-on-Cu type and 563.50 N for Cu-on-Al; and the errors between simulations and tests are within 10%.

7. Conclusion

This paper discusses applying CAE analysis for bonding-strength analysis of Cu-Al heterogeneous laser-stacking process for automotive power lithium-ion battery modules and series-connected electrode sheets; as well as the comparisons with related tests. It is expected to cut costs resulted from experiment try and error, and accumulated key analysis data. Under different Cu-Al heterogeneous laser-stacking process conditions, the simulation analysis can be used to predict the welding bonding-strength, so as to meet a maker's strength target. Thus, the welding-bead bonding-strength simulation method developed in this paper is expected to be applied to subsequent welding conditions; and provide an effective welding bonding-strength analysis method.

Acknowledgments

This paper is sponsored by the MOEA (Ministry of Economic Affairs) from the Technology Development Program No. 109-EC-17-A-25-1581. It is gratefully acknowledged for its successful completion.

References

[1] Shannon, G., and Chen, H. 2009. "Laser Welding of Aluminum and Copper for Battery Welding Applications Using a 500 W Single Mode Fiber Laser." *Journal of Laser Applications* 21: 1015-20.

[2] Xue, Z., Hu, S., Zuo, D., Cai, W., Lee, D., and Kannatey-Asibu, E. 2013. "Molten Pool Characterization of Laser Lap Welded Copper and Aluminum." *Journal of Physics D: Applied Physics* 46: 1-9.

[3] Chopde, R. S., Gadewar, S. P., Khond, M. P., and Rathod, M. J. 2017. "Study on Laser Beam Welding of Copper and Aluminum Joint." *IOSR Journal of Mechanical and Civil Engineering* 23: 65-74.

[4] Hofmann, K., Holzer, M., Hugger, F., Roth, S., and Schmidt, M. 2014. "Reliable Copper and Aluminum Connections for High Power Applications in Electromobility." *Physics Procedia.* 56: 601-9.

[5] Wang, L., Felicelli, S., and Pratt, P. 2008. "Residual Stresses in LENS-deposited AISI 410 Stainless Steel Plates." *Materials Science and Engineering A* 496: 234-41.

[6] Li, C., Wang, Y., Zhan, H., Han, T., Han. B., and Zhao, W. 2010. "Three-Dimensional Finite Element Analysis of Temperatures and Stresses in Wide-band Laser Surface Melting Processing." *Materials and Design* 31: 3366-73.

[7] Li, C., and Wang, Y. 2013. "Three-Dimensional Finite Element Analysis of Temperature and Stress Distributions for In-Service Welding Process." *Materials and Design* 52: 1052-7.

[8] Hartel, U., Ilin, A., Bantel, C., Gibmeier, J., and Michailov, V. 2016. "Finite Element Modeling for the Structural Analysis of Al-Cu Laser Beam Welding." In *Proceedings of the 9th International Conference on Photonic Technologies, Physics Procedia*, pp. 1404-14.